GA 2175 (1199E)

◆ **GENERAL ATOMICS**

PROJECT CONTROL ISSUE SUMMARY

	DOC. CODE	PROJECT	DOCUMENT NO.	REV.
	RGE	30103	PC-000514	0

TITLE: Effect of use of Zirconium Carbide Coatings on the VHTR Core Nuclear Design

CM APPROVAL/ DATE	REV.	PREPARED BY	APPROVALS RESOURCE/ SUPPORT	PROJECT	REVISION DESCRIPTION/ W.O. NO.
ISSUED 2 ▷ DEC 19 2003	0	C. P. Ellis C. P. Ellis 12/18/03	for D. W. McEachern V. Nicolayeff 12/18/03	A. S. Shenoy A.S. Shenoy	Initial Issue W.O. 30103 300 11000

*****SEE LIST OF EFFECTIVE PAGES**

PAGE i OF *

AAA 107 (08/2001)

LIST OF EFFECTIVE PAGES

Page Number	**Number of Pages**	**Revision**
i through v	5	0
3 through 17	15	0
TOTAL NO. OF PAGES:	20	

Table of Contents

List of Tables

List of Figures

Effect of Use of Zirconium Carbide Coatings on the VHTR Core Nuclear Design

1. Background

One of the primary goals of the Very High Temperature Reactor (VHTR) is to provide an outlet temperature of 1000ºC, which is 150ºC higher than that for the reference Gas-Turbine Modular Helium Reactor (GT-MHR) design. The peak fuel temperature in the 600 MW(t), commercial GT-MHR with an 850ºC core outlet temperature is expected to be about 1250ºC for normal operation and less than 1600ºC for depressurized conduction cooldown accidents. A design goal for the VHTR is to optimize the core and plant design such that these peak temperature limits can also be achieved (or nearly so) with a 1000ºC core outlet temperature. Core design changes will permit increased core outlet temperatures without a proportionate increase in peak fuel temperatures during normal operation although some increases in the average fuel and graphite temperatures are expected since the average temperatures largely track the coolant temperatures. Design changes to the reference 600 MW(t) GT-MHR core have been identified which appear to have significant potential for accommodating higher core outlet temperatures; they include fuel shuffling schemes to reduce peaking factors, fixed column orifices to control the flow distribution, modifications to reduce bypass flow, and fuel-element modifications to reduce linear heat rates (Ref. 1). Because of the higher normal operating temperature for the VHTR, the peak fuel temperature during core conduction cool down is expected to be somewhat higher than for the GT-MHR design.

The GT-MHR core utilizes conventional TRISO-coated fuel containing an SiC layer. For the VHTR, the increase in average core temperature may adversely affect the performance of SiC-TRISO fuel. Higher temperatures will affect the thermochemistry of the fuel kernel and will result in increased diffusion rates of fission products from the kernel and through the coating layers. Based on data obtained from a limited number of irradiation tests, there is some evidence that ZrC may be more effective than SiC as a barrier to fission-product release at high temperatures. In this report, the effect of using ZrC-TRISO fuels on the nuclear design of the VHTR is evaluated.

2. Description of Coated Particle Designs using ZrC

Earlier irradiation studies have shown that use of ZrC in coated-particle fuels offers potential performance advantages and superior containment of fission products at high burnup, and at high temperatures (Refs. 2 through 6). The use of ZrC offers the following potential benefits:

- When used as a getter (either mixed with the fuel and/or buffer or as a thin layer surrounding the fuel kernel), oxidation of ZrC can minimize the oxygen potential and reduce CO formation, which is needed to achieve good performance for high burnup fuels;
- Improved retention of fission products within the coating layers;
- Reduced degradation of coating layers as the result of fission-product attack.

However, zirconium will effect the nuclear design of the core, since it has a higher absorption cross-section than either carbon or silicon in the 10^2 to 10^5 eV neutron energy range. Since there

are significant quantities of coatings in the core, the use of zirconium will affect the neutron economy. This effect needs to be considered in the selection of particle designs and in the design of the core.

Three coated particle designs using zirconium carbide have been fabricated and have shown promising performance in irradiation tests (Refs. 2 through 6). These designs are represented schematically in Figure 2-1. The best known of the designs, the TRIZO particle, substitutes a layer of ZrC for the SiC layer in the TRISO particle. Initial TRIZO particle evaluations indicate that it should have superior high temperature performance, suppression of kernel migration, and improved retention of fission products compared to the conventional TRISO particle. A novel design, the UO_2*-2 design uses a thin pyrocarbon seal coating deposited directly on the kernel followed by a thin ZrC coating (both 10 to 15 μm thick). The normal TRISO coating is deposited on this coated kernel. This coating has demonstrated the ability to contain metallic fission and activation products (notably Ag-110m) and to getter oxygen, since kernel migration or pressure-vessel failure was not observed at relatively high burnups. UO_2*-1 uses a modified buffer layer made by co-deposition of low density pyrocarbon containing 5 to 15 wt% ZrC. Use of the three particle designs introduces significantly different amounts of Zr into the core. The mass and number of atoms in the core for the three particle designs is given in Table 2-1.

Figure 2-1: Candidate Designs for Fuel Performance

TRIZO ZrC Barrier	ZrC-Buffer ZrC Getter	UO₂ ZrC Getter and Barrier
Higher Temperature Resists FP Attack Improved FP Retention	Lower CO Pressure Improved FP Retention (Including Ag)	Lower CO Pressure Improved FP Retention (Including Ag)
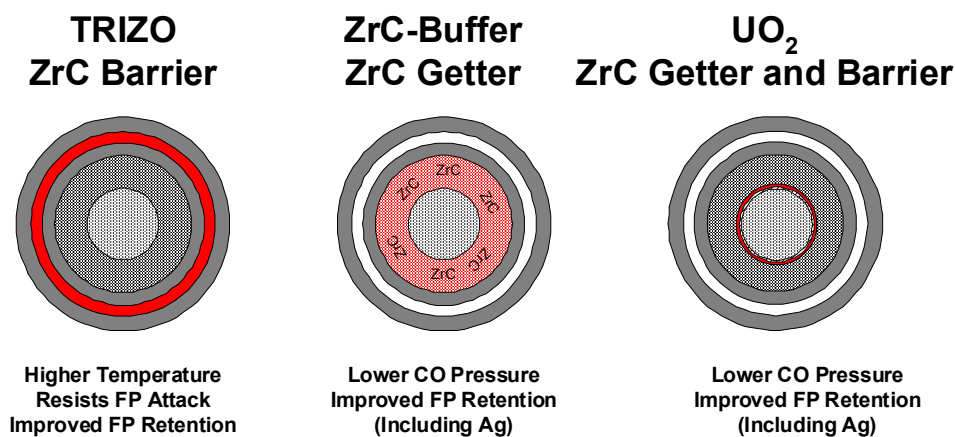
Table 2-1: Relative Mass and Number of Atoms in VHTR for ZrC Particle Designs
(mass Si in core = 2300 kg)

Particle Design	Mass Ratio: Mass i/(Mass Si in SiC-TRISO)		Atom Ratio: Atoms i/(Atoms Si in SiC-TRISO)	
	Si	Zr	Si	Zr
ZrC-TRISO	0	2.5	0	0.78
UO₂*-1 ZrC in buffer	1.1	0.1	1.1	0.03
UO₂*-2 ZrC layer on kernel	1.0	0.26	1.0	0.08

Although ZrC coatings are expected to improve fuel performance, they also affect the nuclear design, including fuel-cycle length. This study provides a preliminary evaluation of the impacts of ZrC particle designs on the VHTR nuclear design and provides recommendations for potential design solutions to achieve a VHTR fuel-cycle length equal to or greater than that for the reference GT-MHR [425 Effective Full Power Days (EFPD)]. For the present study, only the ZrC-TRISO design was evaluated, since it introduces 10 to 25 times more atoms of ZrC into the core than the other ZrC particle designs described above, and hence provides a bounding assessment of the effect of Zr on the VHTR core design.

3.   Nuclear Analysis Methods

To determine the effect of replacing SiC with ZrC in the TRISO particle, the nuclear analysis was be performed as follows:

- Initial cycle cross-sections were developed for both cores (using SiC-TRISO and ZrC-TRISO fuel) using the MICROX code.
- Using the cross-section data, the zero-dimensional GARGOYLE code was used to calculate burnup through the end of cycle 6 (EOC6), to simulate equilibrium-cycle conditions for both cores.
- EOC6 atom densities from GARGOYLE calculations were input to the MICROX code to generate new cross-section sets for both cores. These new sets were utilized by more detailed burnup codes throughout all cycles.
- The 2-D GAUGE code was used to model burnup of the initial cycle for both cores, without simulation of control rod movement. This calculation provides a direct burnup comparison of both cores.
- The GAUGE output results were used to adjust fixed burnable poison (FBP) B-10 loadings to achieve a 425 EFPD cycle length in the ZrC-TRISO core.

4.   Cross-Section Generation

4.1   MICROX – Initial Cycle

Nuclide microscopic cross-section data are typically generated by the MICROX code (Ref. 7). MICROX is an integral transport theory flux spectrum code, which solves the thermalization and neutron slowing down equations on a detailed energy grid for a two-region lattice cell. The two regions are the TRISO fuel particle and the surrounding graphite. The TRISO particle may also be subdivided into two regions - the fuel kernel (grain) and coating layer regions.

MICROX input assumptions:
- Fission neutron sources for both cores are identical.
- Natural zirconium nuclear data.
- ZrC density of 6.73 g/cm^3.
- For uranium-based cores, fuel burnup is slow in the GT-MHR and has little effect on flux distribution during core lifetime. Therefore, a single cross-section set can be used throughout the burnup analysis and no variable particle self-shielding coefficients are needed.

Table 4-1 shows the neutron energy group structure used in the nuclear analysis for both cores. Groups 1 through 5 represent the fast energy range, and the remaining groups are the thermal energy range. Table 4-2 lists the core loadings as input to MICROX.

Table 4-1: MICROX Energy Group Structure

	Group Number								
	1	2	3	4	5	6	7	8	9
Lower Energy (eV)	1.83E5	961	17.61	3.9279	2.38	1.275	0.825	0.13	0

Table 4-2: MICROX Initial Cycle Data

MICROX Region	Nuclide	SiC Core Mass (Kg)	ZrC Core Mass (Kg)	SiC Core Atom Density	ZrC Core Atom Density
Fissile Kernel (LEU)	U-235	595.3	595.3	1.67106E-05	1.67106E-05
	U-238	2411.5	2411.5	6.68316E-05	6.68316E-05
Fertile Kernel (NU)	U-235	18.6	18.6	5.27588E-07	5.27588E-07
	U-238	2625.0	2625.0	7.27454E-05	7.27454E-05
Homogeneously Distributed	B-10	2.0	2.0	1.26361E-06	1.26361E-06
	BIMP	0.0	0.0	2.08762E-08	2.08762E-08
	NBIMP	0.0	0.0	7.19868E-10	7.19868E-10
Coating + Binder	Si-28 or Zr	2272.5	6029.4	5.33818E-04	4.36051E-04
General Distribution	Oxygen	619.9	619.9	2.55609E-04	2.55609E-04
	C-Fuel	29822.2	29644.3	1.63807E-02	1.62830E-02
Moderator	C-Mod	88733.6	88733.6	4.90942E-02	4.90942E-02

Highlighted rows indicate a difference

MICROX cross-section output comparisons are provided in Table 4-3 for only the silicon and zirconium nuclides. The data show the following:

- Transport (in-group scattering) cross-sections are dominant for both nuclides, and are a few orders of magnitude greater for the zirconium core. This is expected because zirconium is the heavier nuclide.
- There are more neutron captures in zirconium, especially in group 3.
- There are slightly more outscatter (out-group scattering) occurrences for the SiC core, more so in group 1.

Table 4-3: MICROX – Initial Cycle

Silicon

Neutrons / Fission	Fission xs	Capture xs	Transport xs	(n,2n) xs	Outscatter xs	Group #
0.00E+00	0.00E+00	4.98E-03	2.65E+00	7.91E-06	2.83E-01	1
0.00E+00	0.00E+00	2.65E-03	2.06E+00	0.00E+00	2.68E-02	2
0.00E+00	0.00E+00	2.55E-03	2.05E+00	0.00E+00	3.13E-02	3
0.00E+00	0.00E+00	8.96E-03	2.02E+00	0.00E+00	8.85E-02	4
0.00E+00	0.00E+00	1.47E-02	2.01E+00	0.00E+00	2.86E-01	5
0.00E+00	0.00E+00	1.94E-02	2.01E+00	0.00E+00	0.00E+00	6
0.00E+00	0.00E+00	2.54E-02	2.01E+00	0.00E+00	0.00E+00	7
0.00E+00	0.00E+00	4.97E-02	2.03E+00	0.00E+00	0.00E+00	8
0.00E+00	0.00E+00	1.03E-01	2.06E+00	0.00E+00		9

Zirconium

Neutrons / Fission	Fission xs	Capture xs	Transport xs	(n,2n) xs	Outscatter xs	Group #
0.00E+00	0.00E+00	7.28E-03	4.55E+00	4.45E-04	6.95E-02	1
0.00E+00	0.00E+00	2.30E-02	8.45E+00	0.00E+00	2.48E-02	2
0.00E+00	0.00E+00	2.44E-01	6.65E+00	0.00E+00	2.90E-02	3
0.00E+00	0.00E+00	1.62E-02	6.15E+00	0.00E+00	8.33E-02	4
0.00E+00	0.00E+00	2.64E-02	6.16E+00	0.00E+00	2.70E-01	5
0.00E+00	0.00E+00	2.23E-02	7.96E+00	0.00E+00	0.00E+00	6
0.00E+00	0.00E+00	2.93E-02	7.95E+00	0.00E+00	0.00E+00	7
0.00E+00	0.00E+00	5.70E-02	7.94E+00	0.00E+00	0.00E+00	8
0.00E+00	0.00E+00	1.18E-01	7.92E+00	0.00E+00		9

Zr/Si cross section ratio

Neutrons / Fission	Fission xs	Capture xs	Transport xs	(n,2n) xs	Outscatter xs	Group #
		1.46	1.71	56.31	0.25	1
		8.67	4.09		0.93	2
		95.56	3.25		0.93	3
		1.81	3.05		0.94	4
		1.80	3.07		0.94	5
		1.15	3.96			6
		1.15	3.95			7
		1.15	3.91			8
		1.15	3.85			9

To support these findings, total absorption cross-section plots for natural zirconium and silicon-28 are provided below in Figure 4-1. Data source is from JENDL-3.2 library.

Figure 4-1: Natural Zirconium and Silicon-28 Total Absorption Cross-Sections
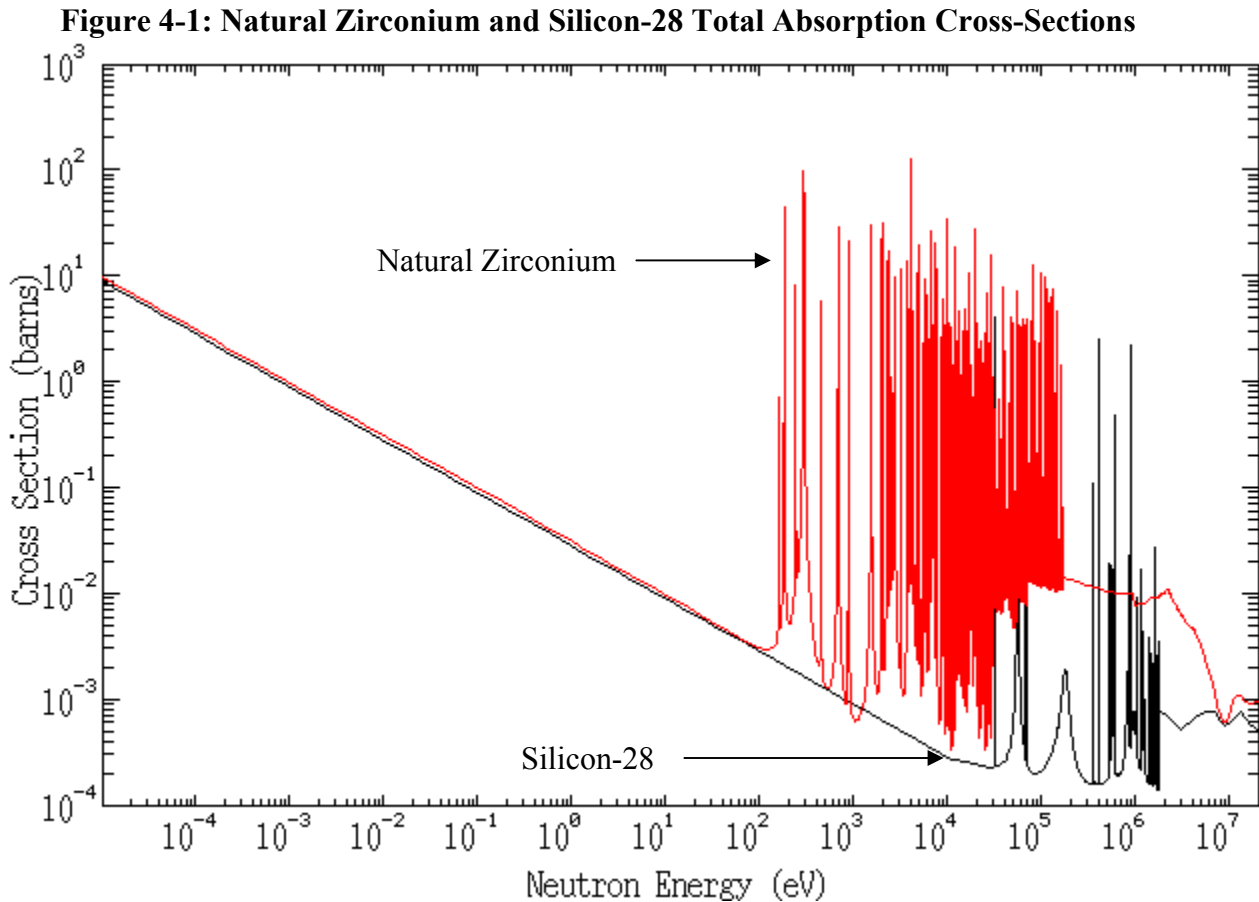
4.2   GARGOYLE

As mentioned in the previous section, the GARGOYLE code was used to generate EOEC atom densities for both cores. GARGOYLE is a zero-dimensional, multigroup depletion code for determining fuel feed requirements for full and/or partial refueling during approach to the equilibrium fuel cycle (Ref. 8.) GARGOYLE has been used primarily to provide fuel cycle depletion and fuel loading input to the design codes and to compute decay heating.

GARGOYLE input assumptions:
- Fission source fractions by energy group are identical for both cores.
- Both cores will be B-10 search-type runs. This can cause inconsistent B-10 loadings for each core, hence inconsistent burnups and nuclide inventories. These differences are neglected since this data is only used in MICROX to generate cross-sections.

Previous work indicates that consistent atom density inputs in the burnup codes are sufficient. Also, as already mentioned, for uranium-based cores fuel burnup is slow and has little effect on flux distribution during the fuel cycle.

For the SiC core, the searched B-10 loadings can be slightly different than the final design reference loadings. These differences may also be neglected as indicated in the previous assumption.

In GARGOYLE, atom densities are input by reload segments A and B. Table 4-4 lists the input loadings data for the initial core and reload segments for both core types.

Table 4-4: GARGOYLE Loadings Data

Cycle	Segment Type	Nuclide	SiC Core Mass (Kg)	ZrC Core Mass (Kg)	SiC Core Atom Density	ZrC Core Atom Density
Initial Cycle	Segment A	U-235 (LEU)	249.2	249.2	1.399E-05	1.399E-05
		U-238 (LEU)	1009.5	1009.5	5.595E-05	5.595E-05
		U-235 (NU)	14.9	14.9	8.500E-07	8.500E-07
		U-238 (NU)	2114.6	2114.6	1.172E-04	1.172E-04
		B-10	*	*	*	*
		BIMP	0.0	0.0	2.076E-08	2.073E-08
		NBIMP	0.0	0.0	7.159E-10	7.147E-10
		Si-28 or Zr	1190.9	3159.7	5.595E-04	4.57021-04
		Oxygen	371.6	371.6	3.064E-04	3.064E-04
		C-Fuel	14684.6	14591.3	1.613E-02	1.60294-02
		C-Mod	44263.8	44263.8	4.898E-02	4.898E-02
	Segment B	U-235 (LEU)	346.1	346.1	1.943E-05	1.943E-05
		U-238 (LEU)	1402.1	1402.1	7.771E-05	7.771E-05
		U-235 (NU)	3.7	3.7	2.052E-07	2.052E-07
		U-238 (NU)	510.4	510.4	2.829E-05	2.829E-05
		B-10	1.7	1.5	2.143E-06	1.900E-06
		BIMP	0.0	0.0	2.099E-08	2.096E-08
		NBIMP	0.0	0.0	7.239E-10	7.228E-10
		Si-28 or Zr	1081.6	2869.7	5.081E-04	4.151E-04
		Oxygen	248.3	248.3	2.048E-04	2.048E-04
		C-Fuel	15137.7	15053.0	1.663E-02	1.654E-02
		C-Mod	44469.8	44469.8	4.921E-02	4.921E-02
Reloads	Segment A and B	U-235 (LEU)	346.1	346.1	1.943E-05	1.943E-05
		U-238 (LEU)	1402.1	1402.1	7.771E-05	7.771E-05
		U-235 (NU)	3.7	3.7	2.052E-07	2.052E-07
		U-238 (NU)	510.4	510.4	2.829E-05	2.829E-05
		B-10	*	*	*	*
		BIMP	0.0	0.0	2.099E-08	2.096E-08
		NBIMP	0.0	0.0	7.239E-10	7.228E-10
		Si-28 or Zr	1081.6	2869.7	5.081E-04	4.151E-04
		Oxygen	248.3	248.3	2.048E-04	2.048E-04
		C-Fuel	15137.7	15053.0	1.663E-02	1.654E-02
		C-Mod	44469.8	44469.8	4.921E-02	4.921E-02

* Search Parameter
Highlighted rows indicate a difference

All cycles were ran for 425 EFPD in both SiC-TRISO and ZrC-TRISO cores. Table 4-5 shows a portion of each GARGOYLE output; namely selected nuclide percent absorptions at EOC6. Notice that for nearly all nuclides, the core absorption distributions for the two core types are within a few percent of each other. The only exception is fertile Am-241 in the fast energy range, but it has little impact because its percent absorptions is less than 0.1%. The calculations also show more absorptions by zirconium in the fast energy range compared to silicon, by a factor of approximately 15. Over the entire energy range, the ratio of neutron absorptions in zirconium to those in silicon is about 2.25. In essence, zirconium behaves like a neutron poison resulting in fewer neutrons absorbed by fuel for the ZrC-TRISO core. Table 4-6 lists actinide atom densities from both the SiC-TRISO and ZrC-TRISO cores at EOC6.

Table 4-5: GARGOYLE - EOC6 - Core Percent Absorptions

Type	Nuclide	Si Fast	Zr Fast	Zr/Si Ratio	Si Thermal	Zr Thermal	Zr/Si Ratio	Si Total	Zr Total	Zr/Si Ratio
Fissile Fuel	U-235	3.98	3.95	0.99	31.26	31.42	1.01	35.24	35.36	1.00
	U-236	0.92	0.91	0.99	0.07	0.07	1.01	0.99	0.98	1.00
	U-238	12.11	12.03	0.99	1.32	1.33	1.01	13.43	13.36	0.99
	Np-237	0.06	0.06	0.99	0.27	0.27	1.00	0.34	0.34	1.00
	Np-239	0.01	0.01	0.99	0.01	0.01	1.00	0.02	0.02	0.99
	Pu-238	0.01	0.01	0.99	0.06	0.06	1.00	0.07	0.07	1.00
	Pu-239	0.37	0.37	0.98	13.92	13.84	0.99	14.30	14.20	0.99
	Pu-240	0.08	0.08	0.99	4.73	4.71	0.99	4.81	4.78	0.99
	Pu-241	0.25	0.24	0.98	3.62	3.60	1.00	3.87	3.85	1.00
	Pu-242	0.08	0.08	0.99	0.02	0.02	1.00	0.10	0.10	0.99
	Am-241	0.00	0.00	0.96	0.06	0.06	0.99	0.06	0.06	0.99
	Am-242M	0.00	0.00	1.00	0.01	0.01	0.99	0.01	0.01	0.99
	Am-243	0.00	0.00	1.00	0.02	0.02	0.99	0.02	0.02	0.99
	Cm-242	0.00	0.00	-	0.00	0.00	1.00	0.00	0.00	1.00
	Cm-243	0.00	0.00	-	0.00	0.00	1.00	0.00	0.00	1.00
	Cm-244	0.00	0.00	-	0.00	0.00	1.00	0.00	0.00	1.00
Fertile Fuel	U-235	0.04	0.04	0.99	0.33	0.33	1.00	0.37	0.37	1.00
	U-236	0.01	0.01	0.99	0.00	0.00	1.00	0.01	0.01	1.00
	U-238	3.74	3.71	0.99	0.49	0.50	1.01	4.23	4.21	1.00
	Np-237	0.00	0.00	1.00	0.00	0.00	1.00	0.00	0.00	0.98
	Np-239	0.00	0.00	1.00	0.00	0.00	1.00	0.01	0.01	1.00
	Pu-238	0.00	0.00	1.00	0.00	0.00	1.00	0.00	0.00	1.00
	Pu-239	0.12	0.11	0.98	4.36	4.33	0.99	4.47	4.45	0.99
	Pu-240	0.02	0.02	0.99	1.48	1.48	0.99	1.51	1.50	0.99
	Pu-241	0.08	0.08	0.98	1.14	1.14	1.00	1.22	1.21	1.00
	Pu-242	0.03	0.02	0.99	0.01	0.01	1.00	0.03	0.03	0.99
	Am-241	0.00	0.00	0.89	0.02	0.02	0.99	0.02	0.02	0.99
	Am-242M	0.00	0.00	1.00	0.00	0.00	1.00	0.00	0.00	1.00
	Am-243	0.00	0.00	1.00	0.01	0.01	0.98	0.01	0.01	0.98
	Cm-242	0.00	0.00	-	0.00	0.00	1.00	0.00	0.00	1.00
	Cm-243	0.00	0.00	-	0.00	0.00	-	0.00	0.00	-
	Cm-244	0.00	0.00	-	0.00	0.00	-	0.00	0.00	-
other	B-10	0.14	0.10	0.76	2.64	2.09	0.79	2.78	2.19	0.79
	Si or Zr	0.05	0.81	15.01	0.53	0.50	0.95	0.58	1.31	2.25

11

Table 4-6: GARGOYLE - EOC6 - Core Atom Densities

Particle Type	Nuclide	Atom Densities		Nuclide	Atom Densities	
		ZrC	SiC		ZrC	SiC
Fissile Particle	U-235	8.131E-06	8.157E-06	Kr-83	1.811E-12	1.814E-12
	U-236	1.940E-06	1.939E-06	Mo-95	7.036E-07	7.028E-07
	U-238	7.447E-05	7.444E-05	Tc-99	6.884E-07	6.879E-07
	Np-237	1.129E-07	1.139E-07	Rh-103	3.285E-07	3.289E-07
	Np-239	1.780E-08	1.791E-08	Rh-105	8.573E-10	8.615E-10
	Pu-238	2.844E-08	2.866E-08	Ag-109	4.036E-08	4.058E-08
	Pu-239	6.192E-07	6.284E-07	Ag-110M	3.445E-10	3.486E-10
	Pu-240	3.097E-07	3.117E-07	I-135	4.446E-10	4.447E-10
	Pu-241	2.418E-07	2.448E-07	Xe-131	2.847E-07	2.844E-07
	Pu-242	1.086E-07	1.092E-07	Xe-135	1.517E-10	1.527E-10
	Am-241	4.498E-09	4.570E-09	Cs-133	7.302E-07	7.294E-07
	Am-242M	1.441E-10	1.463E-10	Cs-134	5.081E-08	5.107E-08
	Am-243	7.187E-09	7.278E-09	Cs-136	5.044E-10	5.053E-10
	Cm-242	2.240E-09	2.253E-09	Nd-143	5.169E-07	5.172E-07
	Cm-243	1.618E-11	1.610E-11	Nd-145	3.978E-07	3.973E-07
	Cm-244	1.264E-09	1.288E-09	Pm-147	1.304E-07	1.300E-07
Fertile Particle	U-235	8.470E-08	8.498E-08	Pm-148M	1.115E-09	1.123E-09
	U-236	2.065E-08	2.063E-08	Pm-148G	8.262E-10	8.273E-10
	U-238	2.728E-05	2.727E-05	Sm-149	1.606E-09	1.619E-09
	Np-237	1.381E-09	1.393E-09	Sm-150	1.469E-07	1.469E-07
	Np-239	5.602E-09	5.634E-09	Sm-151	1.287E-08	1.296E-08
	Pu-238	3.629E-10	3.656E-10	Sm-152	6.711E-08	6.701E-08
	Pu-239	1.913E-07	1.941E-07	Eu-151	9.928E-12	1.007E-11
	Pu-240	9.648E-08	9.704E-08	Eu-152	3.091E-11	3.107E-11
	Pu-241	7.512E-08	7.603E-08	Eu-153	1.496E-08	1.498E-08
	Pu-242	3.434E-08	3.453E-08	Eu-154	3.190E-09	3.207E-09
	Am-241	1.389E-09	1.412E-09	Eu-155	9.707E-10	9.782E-10
	Am-242M	4.437E-11	4.507E-11	NSAG35	9.275E-06	9.249E-06
	Am-243	2.280E-09	2.309E-09	NSAG49	2.484E-06	2.503E-06
	Cm-242	7.002E-10	7.062E-10	B-10	9.170E-08	1.206E-07
	Cm-243	5.105E-12	5.115E-12	B-Nat	2.709E-10	2.763E-10
	Cm-244	4.040E-10	4.116E-10	BIMP	7.228E-10	7.239E-10
				NBIMP	0.000E+00	0.000E+00
				Si or Zr	4.151E-04	5.081E-04
				Oxygen	2.048E-04	2.048E-04
				C-Fuel	1.654E-02	1.663E-02

4.3 MICROX – Equilibrium Cycle

The atom densities given in Table 4-6 were then input to MICROX, and calculations were performed to generate cross-sections for the SiC-TRISO and ZrC-TRISO cores. The MICROX cross sections were not updated to account for changes in initial fuel and B-10 loadings, which is reasonable based on nuclear design calculations performed for previous GT-MHR cores. The same conclusions derived from the Table 4-3 data (for the initial cycle) are also applicable to the EOEC data shown below in Table 4-7. These cross-section sets for the SiC-TRISO and ZrC-TRISO cores were used as input to the burnup codes.

Table 4-7: MICROX – EOEC

Silicon

Neutrons / Fission	Fission xs	Capture xs	Transport xs	(n,2n) xs	Outscatter xs	Group #
0.00E+00	0.00E+00	4.98E-03	2.65E+00	7.91E-06	2.83E-01	1
0.00E+00	0.00E+00	2.65E-03	2.06E+00	0.00E+00	2.69E-02	2
0.00E+00	0.00E+00	2.57E-03	2.05E+00	0.00E+00	3.22E-02	3
0.00E+00	0.00E+00	8.97E-03	2.02E+00	0.00E+00	8.86E-02	4
0.00E+00	0.00E+00	1.47E-02	2.01E+00	0.00E+00	2.87E-01	5
0.00E+00	0.00E+00	1.93E-02	2.01E+00	0.00E+00	0.00E+00	6
0.00E+00	0.00E+00	2.51E-02	1.99E+00	0.00E+00	0.00E+00	7
0.00E+00	0.00E+00	5.08E-02	2.03E+00	0.00E+00	0.00E+00	8
0.00E+00	0.00E+00	1.04E-01	2.07E+00	0.00E+00		9

Zirconium

Neutrons / Fission	Fission xs	Capture xs	Transport xs	(n,2n) xs	Outscatter xs	Group #
0.00E+00	0.00E+00	7.28E-03	4.55E+00	4.45E-04	6.94E-02	1
0.00E+00	0.00E+00	2.30E-02	8.44E+00	0.00E+00	2.49E-02	2
0.00E+00	0.00E+00	2.42E-01	6.65E+00	0.00E+00	2.98E-02	3
0.00E+00	0.00E+00	1.62E-02	6.15E+00	0.00E+00	8.35E-02	4
0.00E+00	0.00E+00	2.64E-02	6.16E+00	0.00E+00	2.70E-01	5
0.00E+00	0.00E+00	2.23E-02	7.95E+00	0.00E+00	0.00E+00	6
0.00E+00	0.00E+00	2.89E-02	7.86E+00	0.00E+00	0.00E+00	7
0.00E+00	0.00E+00	5.82E-02	7.93E+00	0.00E+00	0.00E+00	8
0.00E+00	0.00E+00	1.20E-01	7.95E+00	0.00E+00		9

Zr/Si cross section ratio

Neutrons / Fission	Fission xs	Capture xs	Transport xs	(n,2n) xs	Outscatter xs	Group #
		1.46	1.71	56.26	0.25	1
		8.68	4.09		0.93	2
		94.06	3.25		0.93	3
		1.81	3.05		0.94	4
		1.80	3.07		0.94	5
		1.15	3.96			6
		1.15	3.95			7
		1.15	3.91			8
		1.15	3.84			9

5.   Burnup of Initial Cycle – 2D Model

GAUGE is a 2-D diffusion-depletion code with a triangular spatial mesh (Ref. 9.) The basic geometry unit in GAUGE is a hexagon, which are grouped into 7 hexagons called patches for editing purposes. GAUGE is typically used to perform searches on control rod patterns based upon a desired K-effective.

For this initial study of the ZrC-TRISO core design, GAUGE was used to perform a burnup analysis to determine the effect of zirconium on initial cycle length. The effects of control rod insertion were neglected. Both core types have identical fuel and FBP loadings input to GAUGE. The burnup results are shown in Figure 5-1. The graph clearly shows a consistent poisoning for the zirconium core of about 0.5% K-effective worth as a result of the substitution of Zr for Si. The behavior of K-effective over cycle length is nearly identical for each core type. However, for the ZrC-TRISO core, initial cycle length is somewhat shorter (400 EFPD) because of the increased poisoning of Zr relative to Si .

Figure 5-1: GAUGE Initial Cycle Reference Comparison
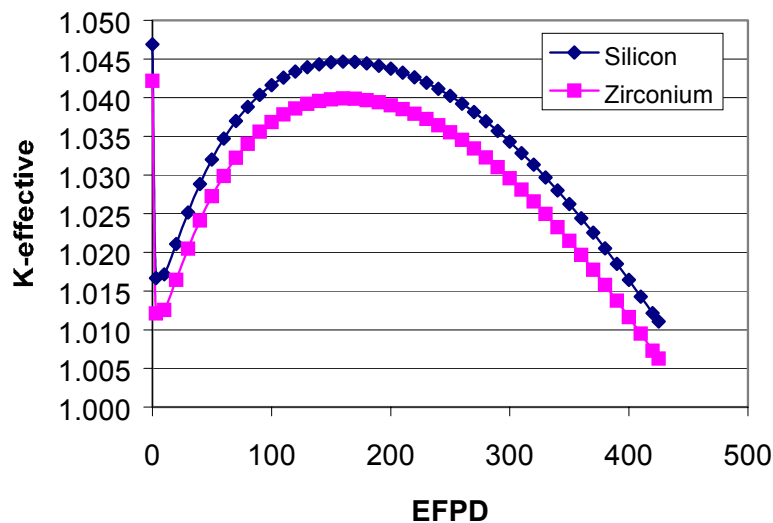
The most obvious approach for extending the ZrC-TRISO core cycle length to 425 EFPD is to remove some FBP (B-10.) GAUGE was used to simulate numerous FBP cases, where both fuel segments were loaded with an equal percent decrease in FBP loadings. The criterion for an optimal new FBP loading was to achieve an end-of-cycle K-effective greater than 1.011.

Figure 5-2: GAUGE Initial Cycle Optimized Comparison
(-12% FBP for Zirconium core)
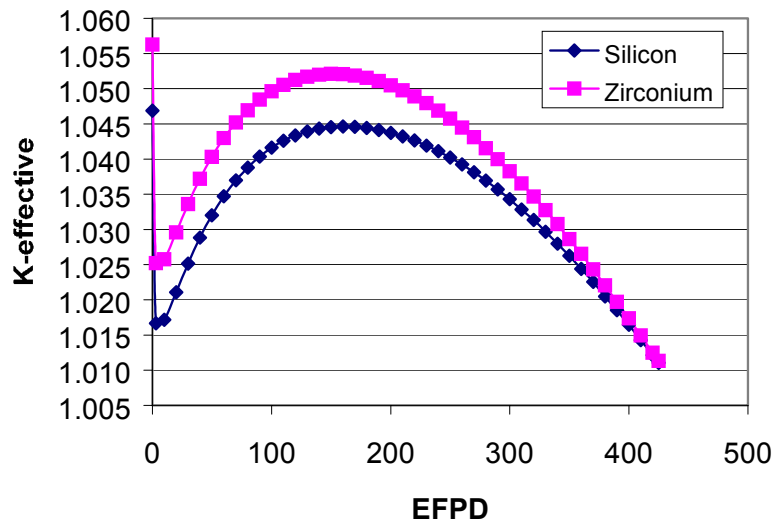
As illustrated in Figure 5-2, the optimal loading for the ZrC-TRISO core is 12% less FBP – essentially the equivalent poison worth of the zirconium. Note the initial increase in K-effective for zirconium followed by a sharper decent to the matching values. This is due to FBP being a burnable poison, while zirconium behaves more like a non-burnable poison. Initially, more fissions are taking place from the reduced FBP. Since there is less FBP in the ZrC-TRISO core, it becomes less effective as a poison sooner in the burnup, which causes K-effective to decline at a faster rate. Because Zr behaves as a non-burnable poison, the initial increase in K-effective is unavoidable. The additional 0.7% K-effective for the ZrC-TRISO core can be accommodated by increasing control rod worths.

6.   Burnup of Reload Cycles – 2D Model

An initial attempt was made to estimate the FBP adjustment needed for the reload cycles. For the SiC-TRISO core, the fuel loadings for the reload cycles are identical to segment B of the initial cycle, while the FBP loadings may change slightly. To simulate the reload cycles, GAUGE was run for both core types, using the optimal FBP for the ZrC-TRISO core, while modeling control rod movement. At 425 EFPD, segment A was replaced with a fresh reload, followed by GAUGE running a straight burnup calculation for cycle 2. The same methodology used for the initial cycle was applied to determine optimal FBP loadings for the ZrC-TRISO core. Results are shown in Figure 6-1.

Figure 6-1: GAUGE Cycle 2 Optimized Comparison
(-14% FBP for Zirconium Core)
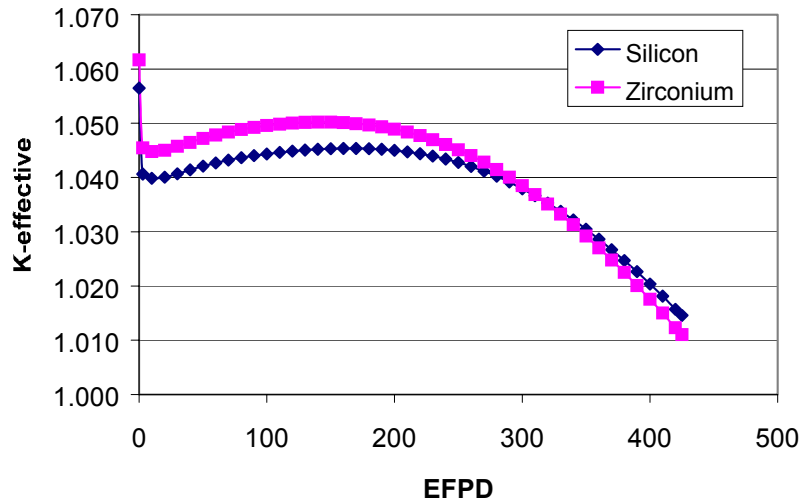
Note that GAUGE predicts an additional 2% decrease in FBP loadings for the ZrC-TRISO core reloads. This can be explained as follows:

- The reductions in FBP loading were assumed to be identical for each segment, However, for the initial cycle, each segment will have slightly different loadings, in terms of atoms of zirconium per atoms of U-235 or U-238. This could cause the segment burnups to be less uniform than that for the SiC-TRISO core, and this effect could be carried over to the reload cycle.
- More importantly, the control rod group insertion patterns were not optimized for all cycles of the ZrC-TRISO core. The optimal pattern will be dependent upon the radial power distributions. The GAUGE calculations performed thus far for the ZrC-TRISO core have assumed the same patterns as those for the SiC-TRISO core.

7. Conclusions

Replacing the SiC layer of the standard GT-MHR TRISO particle with a layer of ZrC poisons the core to an equivalent worth of 12% FBP (0.24 kg B-10) for the initial cycle and 14% FBP (0.23 kg B-10) for the reload cycles. This overall poisoning effect is the net result of the following impacts of Zr on the core design:

- Zr behaves like a non-burnable poison
- In the fast energy range, a factor of 15 greater absorptions in zirconium compared to silicon result in a 1% decrease in uranium absorptions.
- In the thermal energy range, 5% fewer absorptions occur in zirconium compared to silicon, result in 1% more uranium absorptions.
- Over the entire energy range, there are 2.25 more absorptions in zirconium compared to silicon, leading to a 1% decrease in uranium absorptions. This indicates that the

16

fast energy range is the dominating energy group affecting the uranium absorptions. Comparing the uranium cross-sections for both cores confirms that the capture cross-section is less for the ZrC-TRISO core in energy groups 3 and 4. This is a direct result of the additional captures by zirconium in these energy groups, as shown in Table 4-7.

8. Future Work

The following additional studies are recommended:

- Optimization of control rod group insertion patterns by applying radial peaking data, in order to better determine FBP loadings for the ZrC-TRISO core.
- Optimization of FBP loadings by core segment and axial/radial zoning factors.
- The higher core temperatures in the VHTR will allow the use of carbon-carbon composite control rods, which have greater thermal resistance. This would allow control rod placement in the inner reflector and dramatically increase the core power-shaping capabilities. Such a change would require a complete new GAUGE model and burnup analysis.
- Extending the physics modeling to a full three-dimensional core design, and performing assessments of fuel performance and fission product release.
- Apply the detailed three-dimensional peaking factors to the thermal conductivity code POKE to calculate maximum and average fuel and graphite temperatures.
- The final nuclear design output will be used to calculate peak fuel temperatures during a conduction cool down.

9. References

1. MacDonald, P. (editor), "NGNP Point Design - Results of the Initial Neutronic and Thermo-Hydraulic Assessment During FY-03," INEEL/EXT-03-00870, Rev. 1, September 2003.

2. G. H. Reynolds, J. C. Janvier, J. L. Kaae, J. P. Morlevat, "Irradiation Behavior of Experimental Fuel Particles Containing Chemically Vapor Deposited Zirconium Carbide Coatings," *J. Nucl. Mater.,* **62**, 9 (1976).

3. R. E. Bullock, J. L. Kaae, "Performance of Coated UO_2 Particles Gettered with ZrC," *J. Nucl. Mater.,* **115**, 69 (1983).

4. R. E. Bullock, "Fission-Product Release during Post-irradiation Annealing of Several Types of Coated Fuel Particles," *J. Nucl. Mater.,* **125**, 304 (1984)

5. K. Minato, T. Ogawa, T. Koya, H. Sekino, T. Tomita, "Retention of fission product caesium in ZrC-coated Fuel Particles for High-Temperature Gas-Cooled Reactors," *J. Nucl. Mater.,* **279**, 181 (2000)

6. K. Minato, T. Ogwa, K. Fukuda, H. Sekino, I. Kitagawa, N. Mita, "Fission Product Release from ZrC-Coated Fuel Particles during Post-Irradiation Heating at 1800 and 2000 ^{o}C," *J. Nucl. Mater.,* **249**, 142 (1997)

7. P. Wälti and P. Koch, "MICROX – A Two-Region Flux Spectrum Code for the Efficient Calculation of Group Cross Sections", GULF-GA-A10827, April 14, 1972.

8. "MHTGR Core Decay Heat", DOE-HTGR-86-109/Rev. 1, July 7, 1987.

9. R. J. Archibald and P. K. Koch, "A User's and Programmer's Guide to the GAUGE Two-Dimensional Neutron Diffusion Program", GA-A16657, July 1983.